New Insights into Quinine-DNA Binding Using Raman Spectroscopy and Molecular Dynamics Simulations

Supporting Information

David Punihaole,[*,†] Riley J. Workman,[‡] Shiv Upadhyay,[¶] Craig Van Bruggen,[†] Andrew J. Schmitz,[†] Theresa M. Reineke,[†] and Renee R. Frontiera[*,†]

†*Department of Chemistry, University of Minnesota, Minneapolis, Minnesota 55455*

‡*Department of Chemistry and Biochemistry, Center for Computational Sciences, Duquesne University, Pittsburgh, Pennsylvania 15282*

¶*Department of Chemistry, University of Pittsburgh, Pittsburgh, Pennsylvania 15260*

E-mail: punih001@umn.edu; rrf@umn.edu

Computational Methods

Density Functional Theory (DFT) Calculations

DFT calculations for quinine were carried out using Gaussian 16[1] software using the M06-2X[2] functional with the aug-cc-pVDZ[3] basis set. The polarizable continuum model[4] (PCM) was used to implicitly simulate the presence of methanol solvent. In the PCM, the quinine molecule is placed in a cavity within the solvent reaction field, which is defined by methanol's dielectric constant, as well as parameters describing the size of the solvent and other polarization effects.

Normal mode frequencies from the DFT simulations were calculated using the Gaussian Freq calculation type. In this calculation, rotational and translational modes are separated from the internal coordinates, and a Hessian matrix containing mass-weighted second partial derivatives of potential energy with respect to internal displacement is created. This matrix, which contains mass-weighted atomic force constants, is then diagonalized, yielding normal mode frequencies as square roots of the resultant eigenvalues. The calculated frequencies were scaled by a factor of 0.96 to better match the experimental data. This scaling factor was determined empirically by comparing the unscaled, calculated vibrational frequencies to their corresponding experimental frequencies, as shown in Figure S1.

We used the VEDA software[5] to calculate the potential energy distribution (PED) of the normal mode vibrations. Input coordinates, normal mode frequencies, atomic displacements, and the mass-weighted force constant matrix were read into VEDA from the Gaussian log file. A linearly independent set of local vibrational coordinates was introduced, and the percent contribution of each local coordinate to the potential energy of each normal mode was calculated using the atomic displacement and force constant data. The atomic labeling scheme of quinine that we employ in this work is shown in Figure S2.

Molecular Dynamics (MD) Simulation Details

The velocity Verlet integration was used to calculate MD trajectories with NAMD[6] in this work. Time steps of 1 fs and 2 fs were used for quinine and quinine/DNA simulations, respectively. For all simulations, conditions of 300 K and 1 atm were maintained with the Langevin thermostat and piston methods, respectively. Particle mesh Ewald[7] summation was used for full system electrostatics, and bulk solvent was approximated with cubic periodic boundary conditions. Pair-lists were kept for distances <12 Å, non-bonded interactions were cutoff at 10 Å, and a smoothing function was applied at 8 Å.

Molecular Dynamics Simulations of Quinine in Organic Solvents

Quinine was simulated in tetrahydrofuran, dimethylsulfoxide, acetone, acetonitrile, anisole, chloroform, dichloromethane, methanol, and toluene solvents with CHARMM36[8] and Amberff99SB[9] force fields. Both force fields were used for the purposes of comparison, as the calculation of solvent-induced electric fields is a relatively unexplored area in MD. The General Amber Force Field[10] (GAFF) was used to obtain Amber parameters for quinine, as well as the solvents mentioned above. For CHARMM36, the CHARMM Generalized Force Field[11] (CGenFF) provided parameters for quinine, dimethylsulfoxide, tetrahydrofuran, acetone, acetonitrile, methanol, toluene, and anisole. Parameters for chloroform and dichloromethane were not included in CGenFF. They were parameterized using the Force Field Toolkit[12] module of VMD[13]. QM calculations for parameterization were performed with the Gaussian software package.[1]

Quinine was solvated in 40×40×40 Å cubic boxes of solvent molecules, consisting of 517, 719, 538, 471, 477, 600, 347, 933, 359 molecules of acetone, acetonitrile, dimethylsulfoxide, tetrahydrofuran, chloroform, dichloromethane, anisole, methanol, and toluene, respectively. Solvent boxes were created with the appropriate densities using the program Packmol[14].

Topology files for the solvated systems were prepared with VMD[13]. Each system was then minimized for 2000 steps followed by 100 ps of MD equilibration. After equilibration, data-production MD simulations were carried out for 2 ns using a time step of 1 fs. For consistency, an identical simulation protocol was employed for all the solvent systems. Following MD simulations for each solvent, data from the production run was used to determine the local electric field exerted on quinine by the solvent.

Molecular Dynamics Simulations of Quinine in Aqueous Solvent

Single molecules of the mono- and diprotonated forms of quinine were solvated in 64 000 Å^3 boxes of TIP3P[15] water, corresponding to 1931 water molecules, with the Solvate package of VMD[13]. To model an acetate buffer, these systems were neutralized with acetate ions, the parameters of which were included in the CHARMM36 General Force Field[11]. Parameters for the two protonated forms of quinine were generated using the Force Field Toolkit[12] module of VMD[13], which utilizes CGenFF.[11] The two systems of aqueous mono- and diprotonated quinine were energy minimized for 2000 steps, followed by 100 ps of MD equilibration. After equilibration, data production MD simulations were carried out for 2 ns. Afterwards, the local electric field on quinine was calculated from the production data.

Molecular Dynamics Simulations of Quinine-DNA Complexation

Two systems of diprotonated quinine with double helix DNA in acetate buffer were prepared. One system consisted of a DNA duplex constructed of adenine-thymine (A-T) base pairs, while the other system consisted of a duplex with cytosine-guanine (C-G) base pairs. These DNA sequences were chosen because calf thymus DNA is too large to simulate, and these sequences contain stretches of both common base pairs. Coordinates for DNA helices were obtained using the Avogadro software package[16]. Solvated quinine/DNA systems

were then created with VMD[13] using the aforementioned diprotonated quinine models. The two systems were solvated in 379 168 $Å^3$ boxes of TIP3P[15] water composed of 11225 water molecules. Each system contained two diprotonoted quinine molecules, two acetate anions, and 40 sodium ions to maintain a neutral charge. Previously discussed parameters for diprotonated quinine and acetate were used, and CHARMM36 parameters were used for the sodium ions and DNA molecules.

Both quinine/DNA systems were minimized for 2000 steps, and 200 ps of MD equilibration was carried out with force restraints placed on the backbone heavy atoms of the DNA. This was followed by another 200 ps of equilibration with restraints limited to heavy atoms of the first and last residues of the DNA strands to discourage translation of the double helix. The simulations were initialized with quinine 15 Å away from the center of the double helix. During equilibration and production simulations, translation of the quinine molecules was restrained to a cylinder of radius 22 Å surrounding the double helix to maximize sampling of quinine-DNA interactions, similar to the protocol used in work by Roux et al.[17]. Data production MD simulations were carried out for 40 ns. The trajectories from the quinine/DNA production simulations were analyzed with VMD[13], and structures of quinine bound in the minor groove of both the A-T and C-G DNA systems were identified. We determined the persistent hydrogen bonding and π-stacking interactions present in the quinine-DNA bound structures. We define a hydrogen bond as having a heavy atom donor-acceptor distance of $\leq$3.5 Å and bond angles of 180$\pm$35°. We define plane-edge π-stacking interactions using a distance metric of $\leq$5 Å between the edge of the nucleobases to the plane of the quinoline ring of quinine, similar to the analysis of histidine-adenine stacking in Rutledge et al.[18]. The portion of the trajectories with quinine bound were extracted and the local electric field felt by quinine in these structures was determined. Salient quinine-DNA binding interactions were abundant in the coordinate trajectory, occurring in roughly 52 % of trajectory frames for the CG duplex simulation and 45 % of trajectory frames for the AT duplex simulation.

Free energy differences for quinine-DNA binding were calculated with umbrella sampling simulations.

Calculating Electrostatic Force Exerted on Quinine with NAMD

We calculated the local electric field due to solvent electrostatics projected onto the difference dipole vector of the ca. $1370\,\mathrm{cm}^{-1}$ quinoline ring stretching vibration from the MD simulation. To accomplish this, NAMD's PairInteraction utility was used to calculate the electrostatic force exerted by the solvent environment on each heavy atom of quinine's quinoline moiety, atoms 1, 2, 3, 4, 5, 8, 9, 11, 12, and 15 (see Figure S2). This process consisted of running 10 NAMD PairInteraction calculations using the coordinate trajectory from the simulation of interest for the electric field calculation. In each of these PairInteraction calculations, the electrostatic force between the solvent atoms and one heavy atom of quinine's quinoline ring was evaluated for each frame in the trajectory. The solvent environment was defined for all MD simulations as any non-quinine atoms. The simulation protocol described here was used to calculate the electrostatic forces for all systems simulated in this work.

The local electric field vector on atom i is given by the following relationship:

$$\vec{E}_i = \vec{F}_i^{\mathrm{elec}} \cdot q_i^{-1} \tag{S1}$$

where $\vec{F}_i^{\mathrm{elec}}$ is the electrostatic force exerted on atom i by the solvent, and q_i is the partial charge of atom i. To calculate the solvent reaction field for the quinoline stretching mode, the local electric fields on each atom of the quinoline ring were projected onto the normalized difference dipole for the $1370\,\mathrm{cm}^{-1}$ vibration, $\hat{u}_{\mathrm{vib}}$. The average of these projections yielded the effective local electric field, E_{vib}, for one frame of the trajectory:

$$E_{\mathrm{vib}} = \frac{1}{N_{\mathrm{vib}}} \sum_{i}^{N_{\mathrm{vib}}} \vec{E}_i \cdot \hat{u}_{\mathrm{vib}} \tag{S2}$$

where N_{vib} is the number of atoms involved in the vibrations, which in this case is the ten heavy atoms of the quinoline moiety. An ensemble average of E_{vib} was taken over the MD trajectory to calculate the reported MD electric fields. Error bars for the electric field calculation were obtained by computing the standard deviation of the local electric field calculated from the MD simulations, including the ca. 50% of the trajectories that show binding interactions between DNA and quinine. This method of electric field calculation was previously described by Boxer and others[19].

Discrepancy between Electric Fields calculated using CHARMM36, Amberff99sb, and the Onsager Model

Our use of CHARMM36 was motivated by our previous success validating it against Raman measured experimental parameters such as peptide dihedral angles[20,21] and amide carbonyl interaction enthalpies[22]. However, to our knowledge, most studies using MD simulations to calculate local electric fields felt by vibrational probes have employed the Amber force field. Because of this, we repeated our simulations using the Amberff99SB force field to compare to our CHARMM36 results. Overall, we find that the average electric fields calculated using Amberff99SB qualitatively agree with those determined with CHARMM36 (Figure S5b). The Amberff99SB simulations even systematically underestimate the Onsager reaction fields by a factor of ca. 2. However, the correlation between the raw MD calculated electric fields and those calculated using the Onsager model is slightly weaker than CHARMM36 due to the fact that Amberff99SB overestimates the electric field magnitude of chloroform relative to tetrahydrofuran. We attribute the overestimation of the electric field magnitude of chloroform to Amberff99SB's unusually large partial charge parameterized on the chlorine atoms of chloroform.

There are several factors that could lead to the factor of 2 discrepancy between the MD

calculated electric fields with those calculated using the Onsager model. One factor could be due to the crude nature of the Onsager model, which represents the solvent implicitly as a continuum dielectric, whereas the atomistic MD simulations represent the solvent explicitly. Another factor, as noted by Fried et al.[19], is that classical force fields parameterize atoms with fixed partial charges, and do not explicitly take into account electronic polarizability. Consequently, the parameterization of the fixed atomic partial charges could conceivably lead to over- or underestimated electric fields, depending on the system being simulated and the force field being used (see SI for a more detailed discussion). Boxer and coworkers[19] previously suggested that, for carbonyl vibrational probes, local electric fields calculated with MD simulations will be 2-2.5 times larger than external fields determined experimentally. They attribute this scaling factor to the fact that most modern force fields overestimate atomic partial charges to more accurately calculate several condensed phase properties[23]. This overestimation is necessary in part due to the lack of polarizability in fixed charge models. However, we have found no reports in the literature that this necessarily yields artificially strong electrostatic effects that would induce a two-fold increase in the force exerted by a solvent[23]. Instead, we believe the scaling factors applied by Boxer and coworkers are done on an ad hoc basis. The discrepancies observed in the MD calculated electric fields are likely the result of vibrational probe and solvent specific inaccuracies in the force field used. In this work, we observe excellent agreement between experimental and MD-calculated electric fields for the quinoline ring symmetric stretching mode of quinine; however, our MD electric fields are systematically lower than the Onsager model calculated values by a factor of ca. 2. The partial charges of the solute and solvent will play a large role in the accuracy of the electric field calculation, and our results suggest that individual probe/solvent systems yield electric fields that can either over- or under-estimate experimental results.

Calculation of Electric Field from Molecular Dynamics Data

Interatomic forces are not typically printed to any NAMD output; however calculation of the local electric field required us to know the total electrostatic force exerted by the solvent on each ring atom of the quinoline group in quinine for each step of the MD calculations. To do this, NAMD's PairInteraction function was used, which allows one to calculate interaction forces between two groups of atoms. A NAMD calculation can be performed in which each frame of a DCD is run for 0 steps, which just calculates observables and does no MD steps, using the PairInteraction function. This tool prints out the electrostatic *and* Lennard-Jones forces for the interaction, though we were interested in only the electrostatic. We carried out 10 of these PairInteraction NAMD calculations, one for each heavy atom in the quinoline ring of quinine. A configuration file for these NAMD PairInteraction calculations is printed below with comments describing important sections in the file.

```
structure      quinine.2+.ATx22.solv.ion.psf
coordinates    quinine.2+.ATx22.solv.ion.pdb
binCoordinates quinine.2+.ATx22.solv.ion.eq.coor
extendedSystem quinine.2+.ATx22.solv.ion.eq.xsc            # allows calculation to account for PBC

paraTypeCharmm on
parameters     quinine.2+.avogadro.cgenff.par
parameters     par_all36_na.prm
parameters     par_all36_cgenff.prm
parameters     water_ions.par
set temp       0                                           # no temp because no MD simulated here
temperature    $temp

timestep       2.0                                         #
rigidBonds     all                                         #
stepspercycle  10                                          #
exclude        scaled1-4                                   # use same parameters that were
cutoff         10.0                                        # used in the job that generated
switching      on                                          # the trajectory being analyzed
switchdist     8.0                                         #
pairlistdist   12.0                                        #
```

```
PME            on                                          #
PMEGridSpacing 1.0                                         #

pairInteraction       on                                   # activates PairInteraction function
pairInteractionFile   quinine.2+.ATx22.C1.pdb              # reference PDB
pairInteractionCol    B                                    # beta-column in ref PDB identifies groups
pairInteractionGroup1 1                                    # beta-value of 1.00 for group 1
pairInteractionGroup2 2                                    # beta-value of 2.00 for group 2

outputName quinine.2+.ATx22.rerun.C1                       # output name, job writes .coor/.vel/.xsc

set ts 1000                                                # timestep (ts) used to increment log output
coorfile open dcd quinine.2+.ATx22.solv.ion.prod.1.dcd     # DCD coordinate trajectory to be analyzed
while { ![coorfile read] } {                               # loops over frames in DCD
 firstTimeStep $ts                                        # sets timestep for current frame
 run 0                                                    # energy and PairInteraction calculation
 incr ts 1000                                             # increase by DCDfreq from original MD job
}
coorfile close                                             # close DCD
```

The log files from each NAMD PairInteraction calculation contain lines every step that begin `PAIR INTERACTION`. This line contains x, y, z components for both the electrostatic and Lennard-Jones interaction forces calculated with the PairInteraction utility. The electrostatic components for each step were extracted from all 10 log files. A BASH script used to accomplish this is given below.

```
#!/bin/bash
prefix="quinine.2+.ATx22.rerun."
atoms=(C1 C2 C3 C4 C5 C6 C7 C8 C9 N1)
for atom in ${atoms[@]};
do
 logfile=$prefix$atom.log
 datafile=$prefix$atom.pair.dat
 grep "PAIR INTERACTION:" $logfile | awk '{print $10,$11,$12}' > $datafile
done
```

Now that we have the electrostatic force exerted on the 10 ring atoms of the quinoline moiety of quinine, we can perform the final calculation of the local electric field felt by this

set of atoms in quinine. Also needed for this calculation is the unit vector representing the difference dipole of the 1370 cm^{-1} mode. These vectors were obtained from the DCD trajectories by aligning the original difference dipole calculated from QM onto quinine for each frame. The mathematical relationships that make the electric field calculation possible are covered in the Computational Methods section of the main document. This was accomplished with a Python script that will be marked up with explanatory comments.

```
import file_utils as fil                    # import file reading functions
import vector_utils as vect                 # import vector functions

prefix = "quinine.2+.ATx22.rerun."                                      # data file prefix
atoms = ["C1", "C2", "C3", "C4", "C5", "C6", "C7", "C8", "C9", "C10"]   # quinoline atom names
suffix = ".pair.dat"                                                    # data file suffix

Fdata = []                                                              # empty data array to fill
for atom in atoms:                                                      # loop over quinoline atom names
 Fdata.append(fil.Read_Data(prefix+atom+suffix))                       # index data file as xyz array in Fdata
vectors = fil.Read_Data("aligned.dD.vectors.dat")                       # xyz array of dipole derivative (dD) vectors
frames = 4000                                                           # number of data frames
N = 10                                                                  # number of atoms
q = [-0.064, 0.153, 0.014, 0.104, 0.133, -0.113, -0.051, -0.112, 0.22, -0.229]    # charges of quinoline atoms
unitconv = 1.0365*4.184                                                 # convert kcal/(mol*A*q_au) to MV/cm

for i in range(frames):                                          # loop over data frames
 for j in range(N):                                             # for each frame loop over atoms
   vect.Scalar_Product(Fdata[j][i], q[j])                       # product of force vectors and 1/charge for each atom

Esum = 0.0                                                       # instantiate sum of E for all frames

for i in range(frames):                                          # loop over data frames
 Estepsum = 0.0                                                 # instantiate sum of E per data frame
 for j in range(N):                                             # for each frame loop over atoms
   Estepsum += vect.Dot(Fdata[j][i], vectors[i])                # project forces onto dD vectors and add to frame E sum
 Esum += Estepsum/N                                            # add average E per frame to total E sum
Eavg = (Esum/steps)*unitconv                                     # average total E over number of frames and convert units
print("Mean local E-field = "+str(Eavg)+" MV/cm")                # print final E value
```

Umbrella Sampling MD Simulations

Umbrella sampling simulations were prepared from the observed structures of quinine bound in the minor groove of the A-T and C-G DNA systems. Twenty-four equally spaced configurations ranging from the bound state to 12 Å quinine-DNA separation along the y axis were constructed with VMD[13]. Force constraints of $2\,\mathrm{kcal}\cdot\mathrm{mol}^{-1}\cdot\mathrm{\AA}^{-1}$ were applied to the geometrical center of quinine along the separation vector in each window. This force constant value was chosen because it yielded appropriate sampling overlap. Also, $5\,\mathrm{kcal}\cdot\mathrm{mol}^{-1}\cdot\mathrm{\AA}^{-1}$ force constants were applied to motion in the x and z axes to restrain quinine to the quinine-DNA reaction coordinate. Each window was simulated with MD for 200 ps. Free energy differences were calculated from the resulting umbrella sampling data using the weighted histogram analysis method (WHAM[24]).

Molecular Dynamics Simulation Scripts

In this section, example NAMD, BASH, and Python scripts are discussed. Each script can be found in text form in this section, as well as in the GitLab repository:
`https://gitlab.com/workmanr/Quinine_SI_Files`.

All molecular dynamics simulations were run on three 24-core 4-GPU Linux workstations. An example NAMD configuration file for a data production MD simulation used in this work is shown below. This file in particular was used to simulate aqueous diprotonated quinine with double-stranded A–T DNA. Similar configuration files were used for all MD simulations presented in this publication, although the quinine/DNA simulations were the only simulations to include constraints or collective variables, which is why we chose these files to show here.

```
structure      quinine.2+.ATx22.solv.ion.psf              # connectivity of system
coordinates    quinine.2+.ATx22.solv.ion.pdb              # initial coordinates
binCoordinates quinine.2+.ATx22.solv.ion.prod.4.coor      # restart coordinates
```

```
binVelocities  quinine.2+.ATx22.solv.ion.prod.4.vel        # restart velocities
extendedSystem quinine.2+.ATx22.solv.ion.prod.4.xsc        # restart PBC parameters

paraTypeCharmm on                                          # use CHARMM type force field
parameters     quinine.2+.avogadro.cgenff.par              # parameters for non-CGENFF quinine atom types
parameters     par_all36_na.prm                            # parameters for DNA/RNA
parameters     par_all36_cgenff.prm                        # parameters for CGENFF atom types
parameters     water_ions.par                              # parameters for water/ions
set temp       300                                         # temperature variable (NOT A NAMD ARGUMENT)
#temperature    $temp                                      # if no velocities, sets temperature, commented out here

timestep       2.0                                         # 2 fs timestep
rigidBonds     all                                         # heavy atom-hydrogen bonds are rigid
stepspercycle  10                                          # steps between electrostatic force evaluation
exclude        scaled1-4                                   # 1-3 forces are ignored and some 1-4 interactions modified
cutoff         10.0                                        # nonbonded force for pairs with distance < cutoff calculated
switching      on                                          # LJ/electrostatic force smoothed to 0 from switchdist to cutoff
switchdist     8.0                                         # beginning of nonbonded force smoothing function
pairlistdist   12.0                                        # atom pairs with distance < pairlistdist included in pairlists
PME            on                                          # particle Mesh Ewald for full-system electrostatics
PMEGridSpacing 1.0                                         # grid size for PME algorithm

constraints on                                             # harmonic restraints
consref quinine.2+.ATx22.solv.ion.term.ref                 # pdb file specifying atoms to be restrained and positions
conskfile quinine.2+.ATx22.solv.ion.term.k.ref             # pdb file containing force constants to restrain with
conskcol B                                                 # beta-column used for consref and conskref info

langevin         on                                        # Langevin thermostat for temperature control
langevinDamping  1                                         # damping constant gamma
langevinTemp     $temp                                     # target temperature in K
langevinHydrogen off                                       # hydrogen atoms ignored for Langevin dynamics

useGroupPressure     yes                                   # hydrogen group based virial used for pressure/KE evaluation
langevinPiston       on                                    # Langevin piston barostat active
langevinPistonTarget 1.01325                               # target pressure in bar
langevinPistonPeriod 100.0                                 # barostat oscillation time scale in fs
langevinPistonDecay  100.0                                 # barostat damping time scale in fs
langevinPistonTemp   $temp                                 # barostat temperature, set same as langevinTemp
```

```
#cellBasisVector1     68.0  0.0   0.0                    # x-axis PBC length, restart parameters used here, commented
#cellBasisVector2      0.0 68.0   0.0                    # y-axis PBC length, restart parameters used here, commented
#cellBasisVector3      0.0  0.0  82.0                    # z-axis PBC length, restart parameters used here, commented
#cellOrigin            0.0  0.0   0.0                    # xyz PBC center, restart parameters used here, commented
wrapAll               on                                 # consider PBC when writing coordinates

colvars       on                                         # collective variable module
colvarsConfig restraint.cylinder.colvar                  # collective variable configuration file

outputName     quinine.2+.ATx22.solv.ion.prod.5          # output file prefix
restartfreq    1000                                      # how often to write restart files
dcdfreq        1000                                      # how often to write coordinate trajectory
outputEnergies 1000                                      # how often to write energies to log
outputPressure 1000                                      # how often to write pressures to log

run 10000000                                             # run for 10 million steps = 20 fs
```

The constraints section was used to apply restraints that immobilize the terminal residues of the DNA to prevent unfolding or drift. The `.ref` files are PDB files with the β-column altered. NAMD's Collective Variables module was used to restrain the quinine molecules to a cylinder of radius 22 Å surrounding the DNA. Contents of the `.colvar` file are shown below.

```
colvarsTrajFrequency    1000                             # how often to write colvar positions to output
colvarsRestartFrequency 1000                             # how often to write colvar restart files

colvar {                                                 # define a single collective variable
   name restraint1                                      # name of collective variable
   lowerboundary 0.0                                    # minimum value of colvar before restoring force is applied
   upperBoundary 22.0                                   # maximum value of colvar before restoring force is applied
   lowerWallConstant 0.0                                # force constant for restoring force at lowerBoundary
   upperWallConstant 1.0                                # force constant for restoring force at upperBoundary
   distanceXY {                                         # collective variable defined as distance projected on plane
       main {                                           # atoms to be restrained
           atomNumbers { 1407 1408 1409 1410 1411 1414 1415 1417 1418 1421 1422
           1423 1427 1429 1431 1432 1434 1435 1436 1439 1440 1447 1448 1449 }
       }
```

```
      ref {                                              # distance vector between ref atoms and main atoms calculated
          atomNumbers { 12 16 17 19 20 21 683 684 686 688 690 692 715 719 720
          722 723 724 1386 1387 1389 1391 1393 1395 }
      }
      axis (0.0, 0.0, 1.0)                               # distance vector projected onto axis and normalized
   }
}

colvar {                                                  # same definitions as restraint1
 name restraint2
 lowerboundary 0.0
 upperBoundary 22.0
 lowerWallConstant 0.0
 upperWallConstant 1.0
 distanceXY {
   main {
     atomNumbers { 1457 1458 1459 1460 1461 1464 1465 1467 1468 1471 1472 1473 1477
     1479 1481 1482 1484 1485 1486 1489 1490 1497 1498 1499 }
   }
   ref {
     atomNumbers { 12 16 17 19 20 21 683 684 686 688 690 692 715 719 720 722 723 724
     1386 1387 1389 1391 1393 1395 }
   }
   axis (0.0, 0.0, 1.0)
 }
}
```

The collective variable `distanceXY` restrains the `main` selection (here the heavy atoms of quinine) to drift no more than `upperBoundary` (here 22 Å) away from the z-axis coordinate value of the atoms in `ref` (here the backbone atoms of the four terminal residues of DNA). The z-axis coordinate value is specified with the `axis` command.

Experimental Methods

Rheology Measurements

Stock solutions of DNA and quinine were prepared in sodium acetate buffer (pH 4, 0.1 M) at the same concentrations and in the same manner as described for the Raman measurements in the main text ($8\,\mathrm{mg}\cdot\mathrm{mL}^{-1}$ for DNA and $6\,\mathrm{mg}\cdot\mathrm{mL}^{-1}$). The quinine-only and DNA-only solutions were prepared by diluting the stocks solutions with buffer to create a DNA sample at $4\,\mathrm{mg}\cdot\mathrm{mL}^{-1}$ and a quinine sample at $1.5\,\mathrm{mg}\cdot\mathrm{mL}^{-1}$. The quinine/DNA mixture was prepared by combining the stock solutions and additional buffer to yield concentrations equivalent to the quinine-only and DNA-only solutions. These samples were then subject to a variety of tests using a TA AR-G2 rotational rheometer, coupled with the TA Rheology Advantage software with a concentric cylinder sample holder. All samples were analyzed at 23 °C.

The data shown in Figure S7a demonstrates that the quinine solution has the properties of a Newtonian fluid, viz. that its viscosity is independent of shear rate. We note that the apparent increase in viscosity of the quinine solution observed at $100\,\mathrm{s}^{-1}$ is an inertial artifact of the solution. In contrast, the DNA solution exhibits apparent shear thinning, indicating that it behaves as a non-Newtonian fluid[25]. At particularly small shear rates, the Newtonian plateau manifests itself around $0.1\,\mathrm{s}^{-1}$.

Figure S7b demonstrates the linear region in the quinine/DNA mixture occurs from around 1 to just over 10% strain. This test yielded a good indication that 10% strain would be optimal for a frequency sweep test. Figure S7c indicates the mixture containing DNA and quinine has demonstrable increase in the viscoelastic response. The storage modulus (G') is shown to be parallel and larger to the loss modulus (G"). The measurable and noticeable rheological property shift of the solution mixture compared to its constituent parts is further indication of a quinine-DNA interaction.

Fluorescence Measurements and Sample Preparation

Stock solutions of DNA and quinine were prepared in sodium acetate buffer (pH 4, 0.1 M) at the same concentrations and in the same manner as described for the Raman measurements in the main text (vide supra). Due to quinine's sensitivity to quenching by chloride ions, great care was made to ensure any residual chloride ion impurities from the calf thymus DNA was present in equal concentrations in all samples. To control for this, we dialyzed a 5 mL aliquot of the DNA stock solution using a Centrifugal Filter Unit (10 kDa MWCO), which was centrifuged at 3220×g for 172 min. We collected 3.5 mL of the supernatant, which contained any potential residual chloride ions, to prepare the DNA ($4\,\mathrm{mg}\cdot\mathrm{mL}^{-1}$), quinine ($1.5\,\mathrm{mg}\cdot\mathrm{mL}^{-1}$) and quinine-DNA ($1.5\,\mathrm{mg}\cdot\mathrm{mL}^{-1}$) quinine, ($4\,\mathrm{mg}\cdot\mathrm{mL}^{-1}$) sample solutions. From these solutions, we also prepared additional samples by serial diluting 0.1, 0.01, and 0.001×. Aliquots of each solution (100 µL) were placed on black Greiner Cellstar 96 well plates with flat bottoms. The fluorescence spectra (Figure S10) of these solutions were measured using a Synergy H1 Hybrid Reader (BioTek, Winooski, VT). The excitation wavelength was 350 nm and peak emission was monitored at 450 nm.

Table S1: Raman Band Frequencies and Assignments of Quinoline Rings Modes of Quinine

Expt. (cm^{-1})	Calc.[a] (cm^{-1})	Δ[b] (%)	Potential Energy Distribution[c] ($\geq$5% contribution)
1642	1657	0.9	$\nu C^{45}C^{44}$ (73), $\sigma HC^{45}H$ (10), $-\nu C^{44}C^{36}$ (6), $-\delta_{ip}HC^{44}C^{45}$ (6)
1627	1629	0.1	$-\nu C^{8}C^{12}$ (32), $\nu C^{3}C^{8}$ (17), $\delta_{ip}C^{8}C^{12}C^{11}$ (11), $-\delta_{ip}C^{12}C^{11}C^{9}$ (10), $\delta_{ip}HC^{8}C^{12}$ (5)
1596	1614	1.1	$\nu C^{2}C^{1}$ (48), $-\nu N^{15}C^{5}$ (14), $\delta_{ip}HC^{1}C^{5}$ (9)
1582	1587	0.3	$\nu N^{15}C^{5}$ (25), $-\nu C^{5}C^{1}$ (11), $\nu C^{2}C^{3}$ (10), $-\nu C^{3}C^{4}$ (7), $-\delta_{ip}HC^{5}N^{15}$ (7), $-\nu C^{12}C^{11}$ (6), $\nu C^{9}C^{11}$ (5), $\nu C^{12}C^{8}$ (5), $\delta_{ip}C^{4}N^{15}C^{5}$ (5)
1516	1506	0.7	$\nu C^{12}C^{11}$ (12), $-\delta_{ip}HC^{11}C^{12}$ (9), $-\delta_{ip}C^{8}C^{12}C^{11}$ (8), $\delta_{ip}C^{3}C^{8}C^{12}$ (8), $\nu C^{3}C^{4}$ (6), $-\nu C^{5}C^{1}$ (6), $-\delta_{ip}HC^{9}C^{11}$ (5), $\delta_{ip}C^{11}C^{9}C^{4}$ (5), $-\delta_{ip}C^{12}C^{11}C^{9}$ (5)
1437	1412	1.8	$\delta_{ip}HC^{17}H$ (28), $-\nu C^{9}C^{11}$ (18), $-\delta_{ip}HC^{5}N^{15}$ (17), $\nu N^{15}C^{4}$ (6), $\delta_{ip}HC^{8}C^{12}$ (6), $\nu C^{3}C^{8}$ (5)
1370	1373	0.2	$\nu C^{3}C^{4}$ (29), $\nu N^{15}C^{5}$ (13), $-\nu C^{11}C^{12}$ (9), $\delta_{ip}HC^{8}C^{12}$ (7), $\nu C^{2}C^{1}$ (6), $\delta_{ip}HC^{8}C^{12}$ (7), $\delta_{ip}HC^{9}C^{11}$ (6)
1328	1343	1.1	$-\delta_{ip}HC^{5}N^{15}$ (11), $-\nu C^{3}C^{8}$ (9), $\nu C^{11}C^{9}$ (7), $\delta_{ip}HC^{25}C^{26}$ (7), $\nu N^{15}C^{4}$ (5), $-\nu C^{2}C^{3}$ (5), $\delta_{ip}HC^{11}C^{12}$ (5), $\delta_{ip}HC^{21}O^{23}$ (5), $-\delta_{oop}C^{21}C^{2}C^{25}H$ (5)
1310	1296	1.1	$\delta_{ip}HC^{1}C^{5}$ (16), $-\nu N^{15}C^{5}$ (8), $-\nu C^{2}C^{1}$ (8), $-\delta_{ip}HC^{21}O^{23}$ (5)
1228	1249	1.7	$\nu C^{12}O^{16}$ (33), $-\delta_{ip}HC^{9}C^{11}$ (12), $-\nu C^{17}O^{16}$ (6), $\nu C^{4}N^{15}$ (5)
1175	1174	0.1	$\delta_{ip}HC^{8}C^{12}$ (23), $-\delta_{ip}HC^{21}C^{5}$ (15), $\nu C^{2}C^{3}$ (6), $\nu N^{15}C^{4}$ (6), $-\nu C^{12}O^{16}$ (6), $\delta_{ip}HO^{23}C^{21}$ (6), $\nu C^{17}O^{16}$ (5)
823	842	2.4	$\delta_{ip}C^{1}C^{5}N^{15}$ (14), $\chi HC^{1}C^{5}N^{15}$ (9), $-\delta_{ip}C^{4}N^{15}C^{5}$ (6), $\nu C^{28}C^{35}$ (5), $\chi HC^{5}N^{15}C^{4}$ (5), $\chi HC^{11}C^{12}C^{8}$ (5)
769	742	3.5	$-\delta_{ip}C^{8}C^{12}C^{11}$ (7), $\delta_{ip}C^{3}C^{8}C^{12}$ (6), $-\nu N^{15}C^{4}$ (5)
760	726	8.3	$\nu O^{16}C^{12}$ (19), $-\delta_{ip}C^{4}C^{9}C^{11}$ (15), $\delta_{ip}C^{12}C^{11}C^{9}$ (11), $-\delta_{ip}C^{8}C^{12}C^{11}$ (10), $-\nu N^{15}C^{4}$ (8), $\delta_{ip}C^{1}C^{5}N^{15}$ (6), $\delta_{ip}O^{16}C^{12}C^{11}$ (5)

[a] scaled by a factor of 0.96. [b] $\Delta = |\nu_{obs} - \nu_{calc}|/\nu_{obs} \times 100\%$. [c] ν: stretch; δ_{ip}: in-plane deformation; δ_{oop}: out-of-plane deformation χ: torsion

Table S2: Normal Mode Composition of Quinine's Quinoline Ring Symmetric Stretching Mode

Species[a]	Expt. (cm^{-1})	Calc.[b] (cm^{-1})	Δ[c] (%)	Potential Energy Distribution[c] ($\geq$5% contribution)
Q	1370	1377	0.5	νC^3C^4 (29), $\nu N^{15}C^5$ (13), $-\nu C^{11}C^{12}$ (9), $\delta_{ip}HC^8C^{12}$ (7), νC^2C^1 (6), $\delta_{ip}HC^8C^{12}$ (7), $\delta_{ip}HC^9C^{11}$ (6)
QH^+	1370	1371	0.1	νC^3C^4 (23), $\nu N^{15}C^5$ (10), $\delta_{ip}HN^{43}C^{29}$ (10), $-\nu C^{11}C^{12}$ (7), $\delta_{ip}HC^8C^{12}$ (5)
QH^{2+}	1391	1394	0.2	$-\nu C^3C^4$ (11), νC^3C^8 (9), $-\nu C^8C^{12}$ (8), $-\nu C^9C^{11}$ (6), νC^4C^9 (5), $\delta_{oop}C^{21}C^2C^{25}H$ (5)

[a] Q: unprotonated quinine; QH^+: monoprotonated quinine; QH^{2+}: diprotonated quinine. [b] scaled by a factor of 0.96. [c] $\Delta = |\nu_{obs} - \nu_{calc}|/\nu_{obs} \times 100\%$.
[d] ν: stretch; δ_{ip}: in-plane deformation; δ_{oop}: out-of-plane deformation χ: torsion.

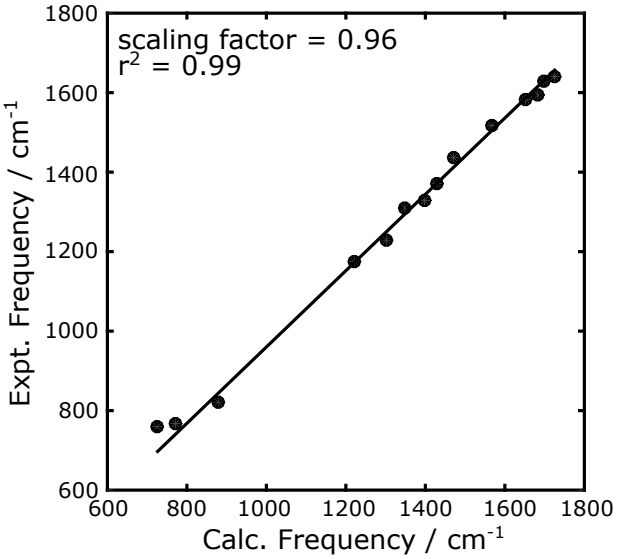

Figure S1: Unscaled calculated (M06-2X/aug-cc-pVDZ) vibrational frequencies in comparison to experimentally measured values for quinine.

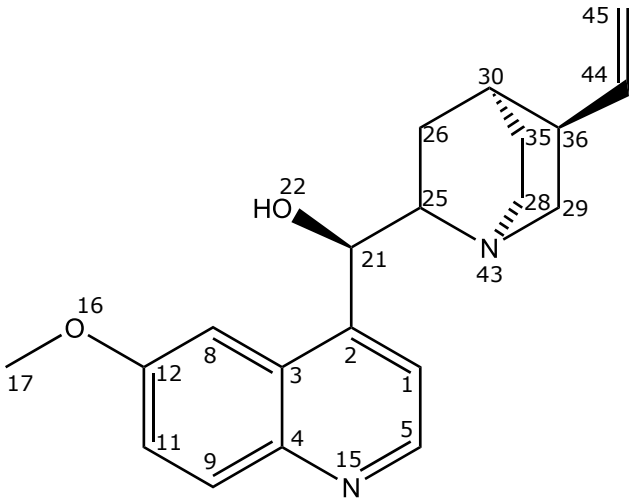

Figure S2: Chemical structure of quinine and the atomic labeling scheme of the heavy atoms used for normal mode analysis in Table SS1.

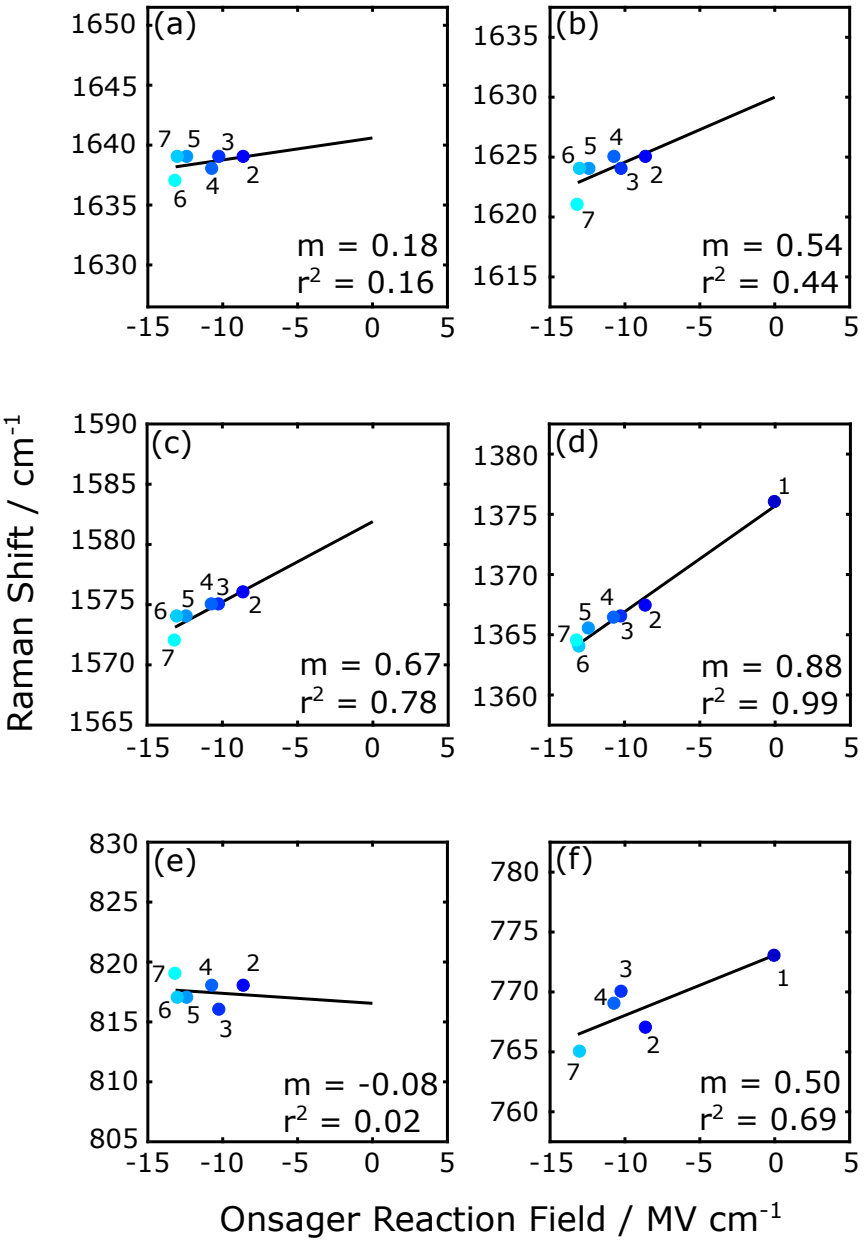

Figure S3: Solvatochromic shift data for prominent quinine Raman modes located at ca. (a) 1640 cm^{-1}, (b) 1630 cm^{-1}, (c) 1580 cm^{-1}, (d) 1370 cm^{-1}, (e) 820 cm^{-1}, and (f) 770 cm^{-1} in different non-aromatic and aprotic solvents. The numbered points denote the following solvents: (1) gas phase; (2) chloroform; (3) tetrahydrofuran; (4) dichloromethane; (5) acetone; (6) acetonitrile; and (7) dimethylsulfoxide. The gas phase frequencies were obtained form Sen et al.[26] The solvatochromic shift data for each mode were least-squares fit to eq. 2, shown in the main text. The slope (m) and coefficient of determination (r^2) values for each mode are reported in each subplot. The units for the reported slopes are $cm^{-1}/MV{\cdot}cm^{-1}$.

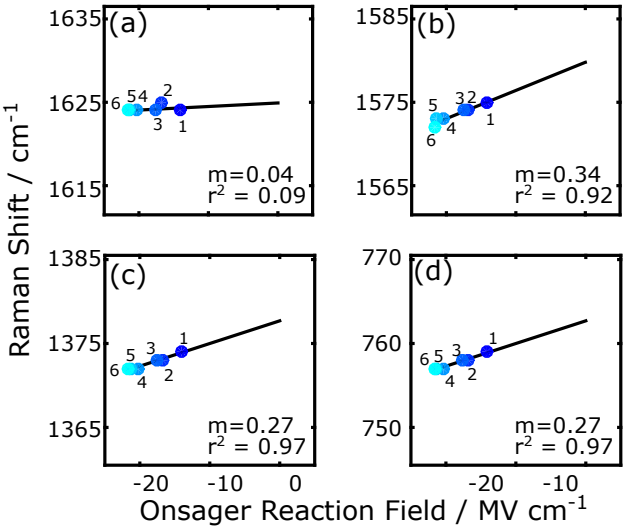

Figure S4: Solvatochromic shift data for prominent quinoline Raman modes located at ca. (a) 1625 cm^{-1}, (b) 1575 cm^{-1}, (c) 1375 cm^{-1}, and (d) 760 cm^{-1} in different non-aromatic and aprotic solvents. The numbered points denote the following solvents: (1) chloroform; (2) tetrahydrofuran; (3) dichloromethane; (4) acetone; (5) acetonitrile; and (6) dimethylsulfoxide. The solvatochromic shift data for each mode were least-squares fit to eq. 2, shown in the main text. The slope (m) and coefficient of determination (r^2) values for each mode are reported in each subplot. The units for the reported slopes are $cm^{-1}/MV{\cdot}cm^{-1}$.

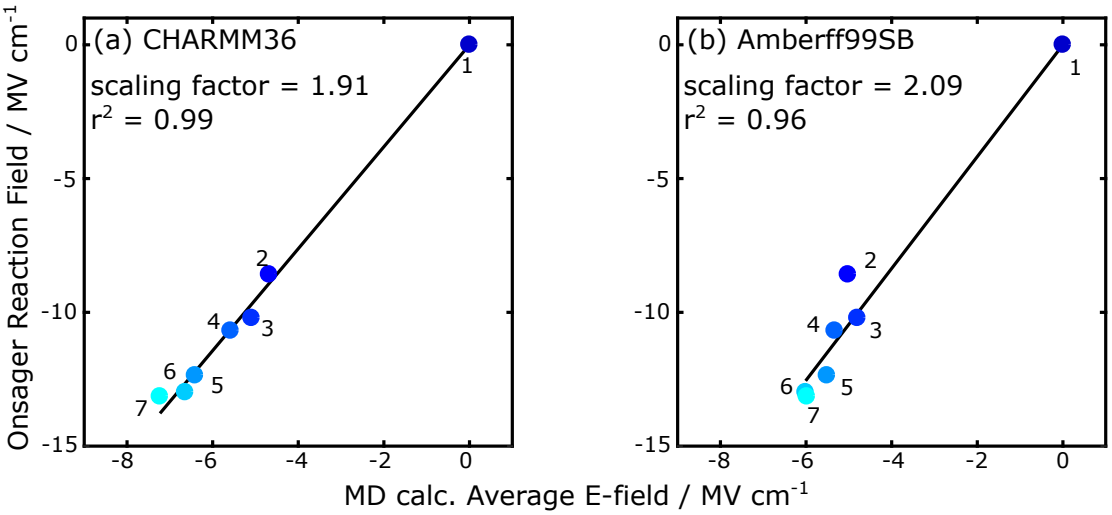

Figure S5: Comparison of average solvent reaction fields calculated using the Onsager model and from atomistic MD simulations with the (a) CHARMM36 and (b) Amberff99SB force fields. The numbered points denote the following solvents: (1) gas phase; (2) chloroform; (3) tetrahydrofuran; (4) dichloromethane; (5) acetone; (6) acetonitrile; and (7) dimethylsulfoxide. Note that, for chloroform, Amberff99SB apparently overestimates the average electric field projected onto quinine's ca. 1370 cm^{-1} mode relative to CHARMM36 due to the unusually large partial charge parameterized on the chlorine atoms. The data were modeled to linear fits to extract scaling factors for the MD calculated electric fields. Both CHARMM36 and Amberff99BS systematically underestimate the solvent reaction fields by a factor of ca. 2 compared to the Onsager model.

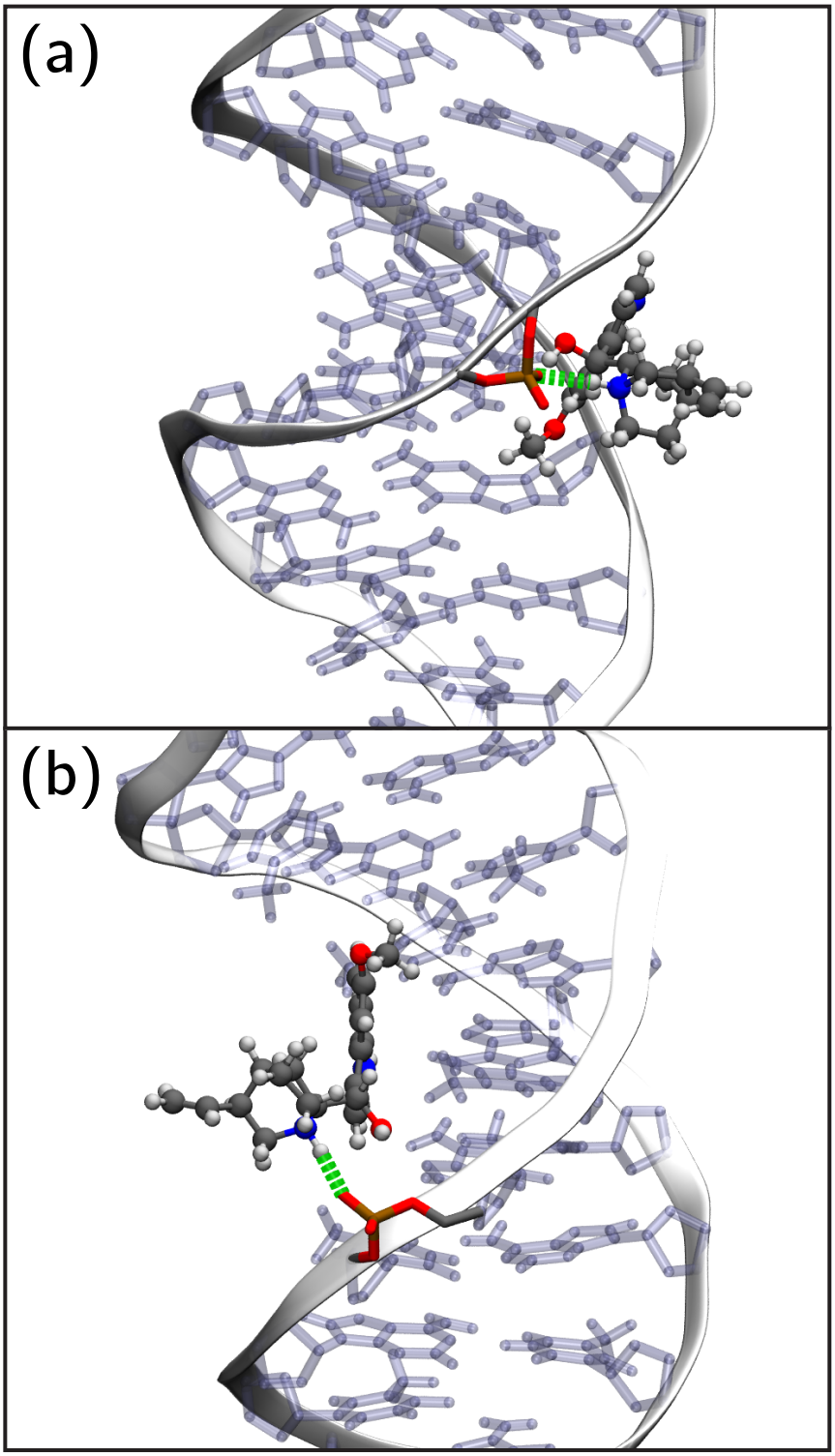

Figure S6: Example of electrostatic interactions between the protonated quinuclidine head group of quinine and the phosphate backbone of DNA for the (a) $(AT)_{11}$ and (b) $(CG)_{11}$ models. The interactions are depicted with dashed green cylinders.

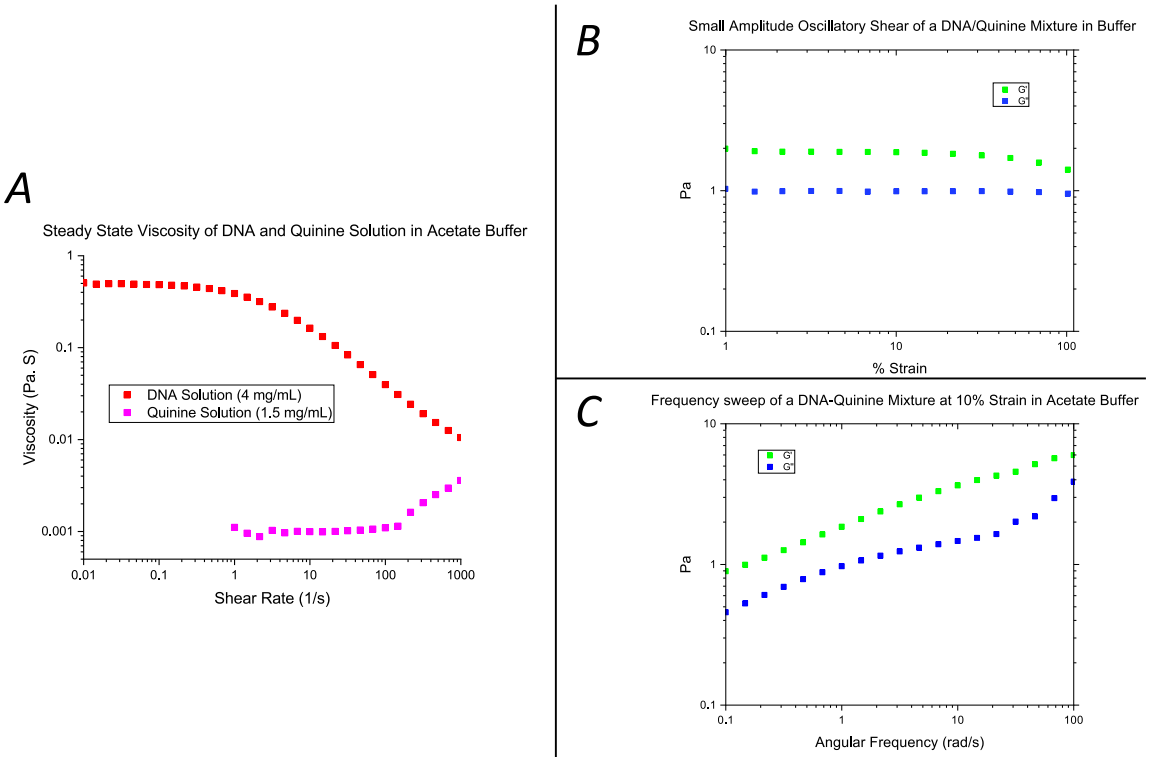

Figure S7: Rhealogy data of quinine and DNA in solution. (a) Stepped steady state viscosity test of DNA and quinine solutions. Solutions were subject to a constant shear rate for 10 seconds with an average of the last 5 seconds used for data collection. (b) Small amplitude oscillatory shear test (SAOS) of a DNA/quinine mixture ($4\,\mathrm{mg}\cdot\mathrm{mL}^{-1}$, $1.5\,\mathrm{mg}\cdot\mathrm{mL}^{-1}$ quinine) in acetate buffer solution. Upon strain shift, there was a 3 second conditioning window, followed by 3 second average sampling windows. Two consecutive measurements within one percent were require for strain progression. (c) Frequency sweep of a DNA-quinine mixture at 10% strain in acetate buffer. Upon frequency shift, there was a 3 second conditioning window followed by 3 second average sampling windows. Two consecutive measurements within one percent were required for a frequency progression.

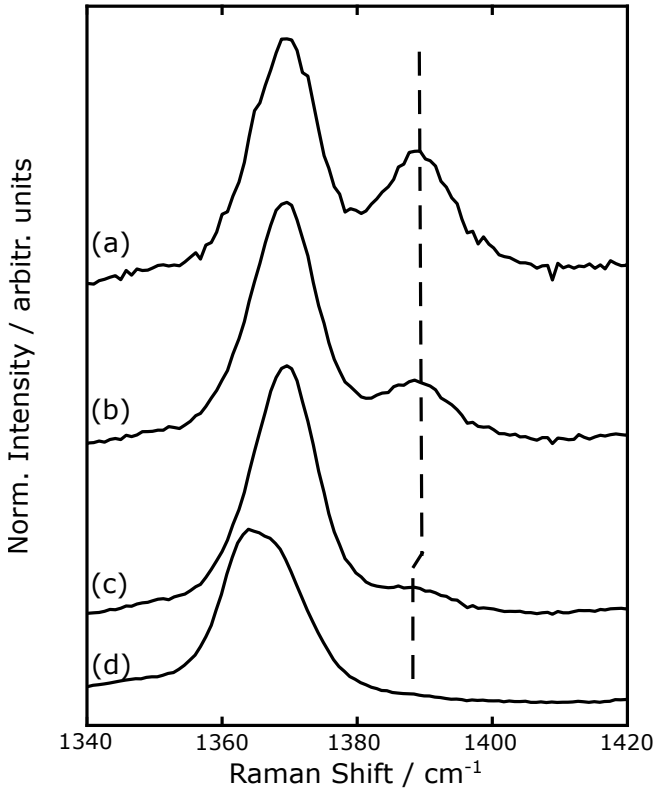

Figure S8: Concentration-dependent changes in the Raman spectra of quinine in 0.1 M sodium acetate buffer. Quinine solutions in (a – c) were prepared at (a) $6.15\,\mathrm{mg}\cdot\mathrm{mL}^{-1}$, (b) $12.3\,\mathrm{mg}\cdot\mathrm{mL}^{-1}$, and (c) $19.4\,\mathrm{mg}\cdot\mathrm{mL}^{-1}$. Solution (b) was close to the saturation point, while solution (c) was super-saturated. The spectrum shown in (d) is of high molecular weight quinine aggregates.

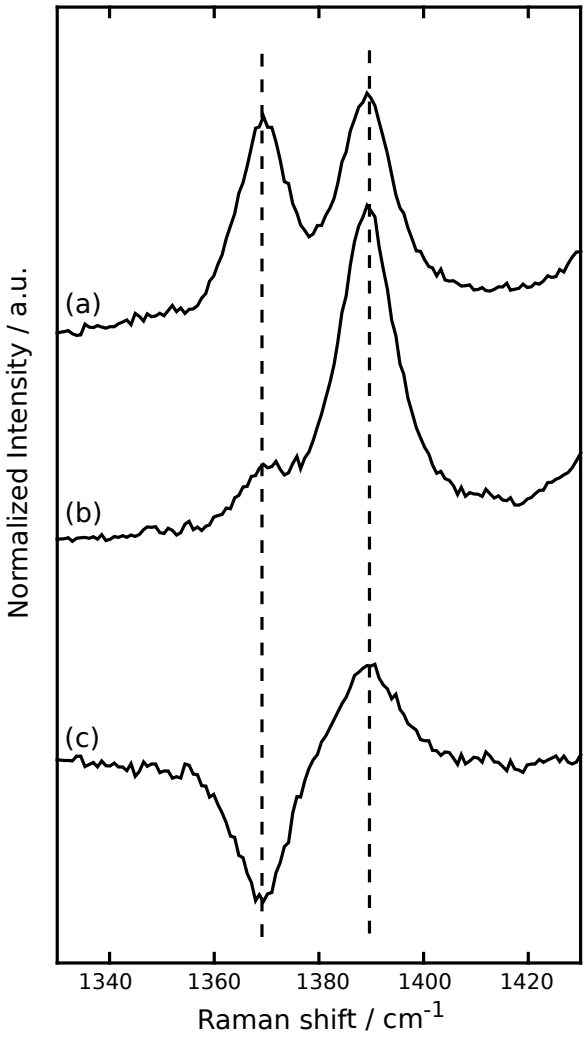

Figure S9: Raman spectra of quinine (a) without Na_2HPO_4 and (b) with 1 M Na_2HPO_4 in 0.1 M sodium acetate buffer (pH 4).

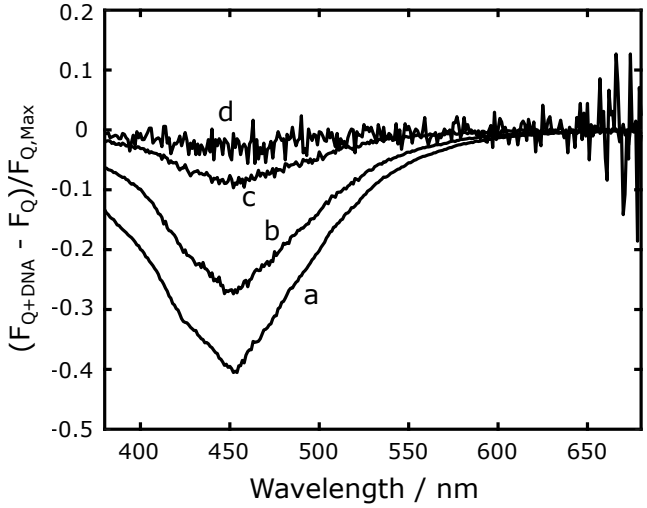

Figure S10: Normalized fluorescence difference spectra of quinine-DNA mixed together in solution. The solution corresponding to the difference spectrum in (a) was prepared at a concentration of $4\,\mathrm{mg}\cdot\mathrm{mL}^{-1}$ DNA and $1.5\,\mathrm{mg}\cdot\mathrm{mL}^{-1}$ quinine. The solutions corresponding to the difference spectra shown in (b), (c), and (d) were of 1:10, 1:100, 1:1000 dilutions, respectively, of the solution prepared in (a).

References

(1) Frisch, M. J.; Trucks, G. W.; Schlegel, H. B.; Scuseria, G. E.; Robb, M. A.; Cheeseman, J. R.; Scalmani, G.; Barone, V.; Petersson, G. A.; Nakatsuji, H. et al. Gaussian16 Revision A.01. 2016; Gaussian Inc. Wallingford CT.

(2) Zhao, Y.; Truhlar, D. G. The M06 Suite of Density Functionals for Main Group Thermochemistry, Thermochemical Kinetics, Noncovalent Interactions, Excited States, and Transition Elements: Two New Functionals and Systematic Testing of Four M06-Class Functionals and 12 Other Functionals. *Theor. Chem. Acc.* **2008**, *120*, 215–241.

(3) Dunning Jr., T. H. Gaussian Basis Sets for Use in Correlated Molecular Calculations. I. The Atoms Boron through Neon and Hydrogen. *J. Chem. Phys.* **1989**, *90*, 1007–1023.

(4) Tomasi, J.; Mennucci, B.; Cammi, R. Quantum Mechanical Continuum Solvation Models. *Chemical Reviews* **2005**, *105*, 2999–3094.

(5) Jamróz, M. H. Vibrational Energy Distribution Analysis (VEDA): Scopes and Limitations. *Spectrochim. Acta A.* **2013**, *114*, 220 – 230.

(6) Phillips, J. C.; Braun, R.; Wang, W.; Gumbart, J.; Tajkhorshid, E.; Villa, E.; Chipot, C.; Skeel, R. D.; Kal, L.; Schulten, K. Scalable Molecular Dynamics with NAMD. *J. Comput. Chem.* **2005**, *26*, 1781–1802.

(7) Darden, T.; York, D.; Pedersen, L. Particle Mesh Ewald: An N·log(N) Method for Ewald Sums in Large Systems. *J. Chem. Phys.* **1993**, *98*, 10089–10092.

(8) Huang, J.; MacKerell Jr., A. D. CHARMM36 All-Atom Additive Protein Force Field: Validation Based on Comparison to NMR Data. *J. Comput. Chem.* **2013**, *34*, 2135–2145.

(9) Hornak, V.; Abel, R.; Okur, A.; Strockbine, B.; Roitberg, A.; Simmerling, C. Comparison of Multiple Amber Force Fields and Development of Improved Protein Backbone Parameters. *Proteins.* **2006**, *65*, 712–725.

(10) Wang, J.; Wolf, R. M.; Caldwell, J. W.; Kollman, P. A.; Case, D. A. Development and Testing of a General Amber Force Field. *J. Comput. Chem.* **2004**, *25*, 1157–1174.

(11) Vanommeslaeghe, K.; Hatcher, E.; Acharya, C.; Kundu, S.; Zhong, S.; Shim, J.; Darian, E.; Guvench, O.; Lopes, P.; Vorobyov, I. et al. CHARMM General Force Field: A Force Field for Drug-like Molecules Compatible with the CHARMM All-Atom Additive Biological Force Fields. *J. Comput. Chem.* **2010**, *31*, 671–690.

(12) Mayne, C. G.; Saam, J.; Schulten, K.; Tajkhorshid, E.; Gumbart, J. C. Rapid Parameterization of Small Molecules using the Force Field Toolkit. *J. Comput. Chem.* **2013**, *34*, 2757–2770.

(13) Humphrey, W.; Dalke, A.; Schulten, K. VMD: Visual Molecular Dynamics. *J. Mol. Graph. Model.* **1996**, *14*, 33 – 38.

(14) Martinez, L.; Andrade, R.; Birgin, E. G.; Martinez, J. M. PACKMOL: A Package for Building Initial Configurations for Molecular Dynamics Simulations. *J. Comput. Chem.* **2009**, *30*, 2157–2164.

(15) Jorgensen, W. L.; Chandrasekhar, J.; Madura, J. D.; Impey, R. W.; Klein, M. L. Comparison of Simple Potential Functions for Simulating Liquid Water. *J. Chem. Phys.* **1983**, *79*, 926–935.

(16) Hanwell, M. D.; Curtis, D. E.; Lonie, D. C.; Vandermeersch, T.; Zurek, E.; Hutchison, G. R. Avogadro: An Advanced Semantic Chemical Editor, Visualization, and Analysis Platform. *J. Cheminformatics.* **2012**, *4*, 17.

(17) Allen, T. W.; Andersen, O. S.; Roux, B. Ion Permeation through a Narrow Channel: Using Gramacidin to Ascertain All-Atom Molecular Dynamics Potential of Mean Force Methodology and Biomolecular Force Fields. *Biophys. J.* **2006**, *90*, 3447–3468.

(18) Rutledge, L. R.; Durst, H. F.; Wetmore, S. D. Evidence for Stabilization of DNA/RNA-Protein Complexes Arising from Nucleobase-Amino Acid Stacking and T-Shaped Interactions. *J. Chem. Theory Comput.* **2009**, *5*, 1400–1410.

(19) Fried, S. D.; Bagchi, S.; Boxer, S. G. Measuring Electrostatic Fields in Both Hydrogen-Bonding and Non-Hydrogen-Bonding Environments Using Carbonyl Vibrational Probes. *J. Am. Chem. Soc.* **2013**, *135*, 11181–11192.

(20) Punihaole, D.; Workman, R. J.; Hong, Z.; Madura, J. D.; Asher, S. A. Polyglutamine Fibrils: New Insights into Antiparallel β-Sheet Conformational Preference and Side Chain Structure. *J. Phys. Chem. B.* **2016**, *120*, 3012–3026.

(21) Punihaole, D.; Jakubek, R. S.; Workman, R. J.; Marbella, L. E.; Campbell, P.; Madura, J. D.; Asher, S. A. Monomeric Polyglutamine Structures That Evolve into Fibrils. *J. Phys. Chem. B* **2017**, *121*, 5953–5967.

(22) Punihaole, D.; Jakubek, R. S.; Workman, R. J.; Asher, S. A. Interaction Enthalpy of Side Chain and Backbone Amides in Polyglutamine Solution Monomers and Fibrils. *J. Phys. Chem. Lett.* **2018**, *9*, 1944–1950.

(23) MacKerell Jr., A. D. Empirical Force Fields for Biological Macromolecules: Overview and Issues. *J. Comput. Chem.* **2004**, *25*, 1584–1604.

(24) Grossfield, A. WHAM: The Weighted Histogram Analysis Method, Version 2.0.9. `http://membrane.urmc.rochester.edu/content/wham`.

(25) Quemada, D. Rheology of Concentrated Disperse Systems II. A Model for Non-Newtonian Shear Viscosity in Steady Flows. *Rheologica Acta* **1978**, *17*, 632–642.

(26) Sen, A.; Bouchet, A.; Lepre, V.; Le Barbu-Debus, K.; Scuderi, D.; Piuzzi, F.; Zehnacker-Rentien, A. Conformational Analysis of Quinine and Its Pseudo Enantiomer Quinidine: A Combined Jet-Cooled Spectroscopy and Vibrational Circular Dichroism Study. *J. Phys. Chem. A*. **2012**, *116*, 8334–8344.